Polarimetric signatures in winter storms

(Matthew Kumjan, Heather Reeves, and Alexander Ryzhkov)

I. Introduction

Over the past year, work has continued to identify repetitive polarimetric signatures associated with various microphysical processes in winter storms. Analyses of numerous case studies have revealed several such signatures, including 1) a low-level enhancement in Z_{DR} that appears to be related to the refreezing of melted or partially melted hydrometeors, 2) downward excursions of the bright band to the surface resulting in localized regions of heavy, wet snow, 3) plumes of high Z_{DR} associated with embedded updrafts and possibly also related to the generation of supercooled liquid water, 4) regions of high Z_{DR} and K_{DP} that are believed to be associated with dendritic growth and/or ice crystal generation, and 5) an apparent tendency for Z_{DR} in the snow region to increase upon the onset of storm decay as regions of dry, aggregated snow (characterized by low Z_{DR}) are replaced by pristine ice crystals (characterized by high Z_{DR}). First three types of polarimetric signatures (1 – 3) are described herein in more detail.

II. Refreezing signature

2. 1. Refreezing Signature: 30 November 2006 Case

The winter storm on 29 – 30 November 2006 began with convective thunderstorms producing rain, followed by freezing rain after the surface temperatures behind the cold front dropped below freezing, then turning to "thundersleet." The ice pellets continued for several hours, before finally turning to snow at the end of the storm. During the analysis shown herein, the surface precipitation was sleet in Norman, and several nearby National Weather Service surface stations reported ice needles.

The melting layer "bright band" signature is clearly evident in all polarimetric radar variables at a range of ~ 20 km to the south and east of the radar, and about 15 km to the north and west of the radar. The asymmetry of the feature is indicative of colder air (and thus lower ML heights) to the west and north of the radar. An inner ring of enhanced Z_{DR} is evident at a range of about 5 km and is symmetric about the center of the radar. This is indicated in Fig. 1 as the "secondary bright band'" and is the signature associated with refreezing. This feature is associated with an enhancement in Z_{DR}, a decrease in ρ_{hv} and Z_H, and an increase in K_{DP}. To the northwest of the radar, at the periphery of the echo is a region of strongly enhanced Z_{DR} collocated with reduced ρ_{hv}. This is indicative of pristine ice crystals or dendrites growing at the top of the cloud.

The polarimetric radar variables in the refreezing signature imply the presence of slender ice crystals such as columns or needles oriented with their major axis approximately in the horizontal. To obtain a quasi-vertical profile of the polarimetric variables through the refreezing

signature, data from 4 elevation angles (4.3 – 7.6°) are used. Each radial from a 180° sector to the east of the radar from the 1358 UTC volume scan is used to construct a median profile for each variable (Figs. 2-5). These can be compared to the 12 UTC Norman sounding temperature and dewpoint temperature (Fig. 6).

The median profiles from Z_H show a pronounced decrease towards the ground starting at about 1100 m, until it levels off near ~750 m. All four elevation scans display decreases on the order of 6-7 dB, which is consistent with the change in dielectric of liquid water drops to ice pellets as the freezing process occurs. The "refreezing zone" is confined to a shallow layer, in agreement with the theoretical model of Kumjian et al. (2010). Beneath the refreezing layer, the profiles are nearly roughly constant in height. Above the refreezing layer, a secondary maximum is best seen in the 7.6° scan (blue curve), associated with the traditional melting layer "bright band" signature, centered at about 2300 m AGL. This corresponds to above-freezing temperatures (Fig. 6). Note that the decrease in Z_H associated with refreezing begins at approximately 1100 m, which corresponds to a temperature just below freezing. It should be noted that the observed sounding is taken about 3 hours before the radar observations, so the temperature profile may have changed in the intervening time.

The profile of Z_{DR} (Fig. 3) again displays two maxima, one aloft associated with the melting layer bright band, and an equally impressive enhancement at low levels (centered at about ~950 m). This secondary maximum appears to be related to the refreezing process. Indeed, it is collocated with the gradient of Z_H in the refreezing zone, with the maximum in Z_{DR} located only a few hundred meters above the temperature minimum in the sounding. The positive Z_{DR} perturbation is of about 0.5 dB in magnitude and is approximately confined to the refreezing zone, or the layer containing the Z_H gradient. The Z_{DR} beneath the refreezing zone continues to decrease towards the ground. Above the refreezing zone, Z_{DR} values are approximately constant, with an average around 0.5 dB. The Z_H and Z_{DR} values in this warm layer (~30 dBZ and ~0.5 dB, respectively) are in remarkable agreement with the expected values for rainfall in Oklahoma by Cao et al. (2008).

The median K_{DP} values (Fig. 4) display substantial variability with height above about 1200 m. Below that level, values are constant at 0 below 500 m and increase in the layer from 500 m to 1000 m. An increase in K_{DP} is expected for horizontally elongated crystals but not for ice pellets. However, it is difficult to interpret K_{DP} as computed in this case: the low Z_H values mean heavy filtering of phiDP is used to compute K_{DP}, which may smooth out some details.

The vertical profiles of ρ_{hv} shown in Fig. 5 display the classic depression associated with the melting layer, where values are as low as ~0.94 to 0.96. Above and below the melting layer, values are quite high, also as expected. However, a slight depression is evident in the profile starting at about 1000 m in height, again at the level of the refreezing zone. This decrease may be attributable to the collocation of multiple hydrometeor species, including partially frozen

drops, ice pellets, and ice crystals. The data below 500 m are contaminated by ground clutter and should not be trusted.

Especially in the top part of this refreezing layer, relatively warm temperatures with water-saturated conditions would certainly promote the presence of supercooled liquid water droplets. Such droplets are necessary for riming of frozen particles, such as that inferred by "bumps" on ice pellets collected at the surface in Stewart and Crawford (1995). Riming is also a necessary condition for the H-M process.

We suggest that a "coincidental" presence of ice crystals (e.g., from depositional growth in the cloud) is unlikely because the presence of radar-detectable precipitation particles seems necessary to produce the refreezing signature (Fig. 7). In areas where there are no appreciable precipitation echoes aloft, the low-level Z_{DR} enhancement is also absent. Thus, it seems likely that the ice crystals are produced because of the presence of precipitation; in other words, an ice multiplication/enhancement process is most likely occurring.

2.2 Refreezing signature. 27 January 2009 case

A winter storm struck most of Oklahoma on 26-28 January 2009, producing a light icing owing to freezing drizzle, followed by several inches of ice pellets across the central part of the state. Ice pellets were the dominant precipitation type through much of 27 January. KOUN collected data continuously throughout the event, offering a high-quality dataset of winter precipitation.

Figure 8 is a PPI display of Z_H and Z_{DR} from about 2005 UTC, when ice pellets were ongoing across much of the central part of the state. At the periphery of the precipitation echo, patches of higher Z_{DR} collocated with low Z_H are indicative of anisotropic ice particles, likely pristine crystals such as dendrites or needles. A classic melting layer bright band signature is present in both Z_H and Z_{DR}, encircling the radar at a slant range of about 45 km (i.e., peak Z_H is at about 1700 m AGL). Note that the regions of enhanced Z_H in the bright band are located beneath areas of Z_{DR} closer to 0 dB, possibly indicative of larger snow aggregates falling into the melting layer. Beneath the melting layer, a secondary region of enhanced Z_{DR} (coincident with a local maximum in Z_H) is found encircling the radar at a range of about 10 km.

As in the analysis of the previous case on 30 November 2006, vertical profiles shown herein are constructed by taking the median value of each radar variable (Z_H, Z_{DR}, and ρ_{hv}) at each range gate over all azimuths. Because the data are "super-resolution," 720 azimuths are included in the computation of the median profiles. Taking the median over all azimuths helps filter out local variations, but should only be applied when precipitation is widespread and relatively uniform. For each of the vertical profiles shown below, the 3.3° elevation angle is used.

Figure 9 displays these quasi-vertical profiles along with the temperature and dewpoint temperature profiles observed from the 1200 UTC Norman sounding on 27 January and the 0000 UTC sounding on 28 January. Note that neither sounding is truly representative of the thermodynamic environment of these quasi-vertical profiles of the radar variables; the true temperature and dewpoint temperatures are expected to lie between these two soundings. Both show a warm layer, with temperatures peaking about 1.4 km AGL. Beneath this warm nose, the environment is saturated with respect to water (supersaturated with respect to ice), and the temperature decreases sharply towards the ground. On both observed profiles, the temperature drops below -5 °C at about 700 m AGL. Beneath this level, conditions are moist but not saturated with respect to water (at least according to the soundings). On the 0000 UTC sounding, the temperatures in this near-surface layer (-10 to -11 °C) and relative humidities (~90%) are such that ice saturation is possible. The "kink" in the 0000 UTC temperature profile at about 600 m AGL could be an indication of warming owing to ongoing microphysical processes: freezing (release of latent enthalpy of fusion) or depositional growth of the newly-generated needles (release of latent enthalpy of vaporization). Further calculations may elucidate which process could contribute more to such warming. Unfortunately, the coarse resolution of the sounding leaves the true degree of warming uncertain.

Quasi-vertical profiles of Z_{DR} display two maxima: one at about 1.8 km AGL, and a larger peak just below 500 m AGL. The first of these is associated with the melting layer bright band. The near-surface peak is the "refreezing signature." Note that it is present for the entire 30-minute period of analysis, though its magnitude changes from scan to scan. In the profiles of Z_H, a well-defined maximum is evident between1.5-2.0 km AGL, associated with the melting layer. Beneath this nose, Z_H values increases (especially in the later scans) towards the ground slightly, until it drops off sharply at about 500 m AGL. The magnitude of this drop off is approximately 6-7 dB, which is consistent with a change in dielectric from liquid drops to ice pellets. The sharp gradient in Z_H is also consistent with the theoretical model of freezing drops by Kumjian et al. (2010). Note that this sharp decrease in Z_H is coincident with the increase in Z_{DR} in the refreezing signature.

When comparing the different profiles, we notice that the 1934 UTC scan displays lower Z_H values beneath the melting layer than the other three scans (e.g., in the 500 – 1500 m layer). Z_{DR} values beneath the bright band are also slightly lower for the 1934 UTC scan, and the magnitude of the refreezing signature is 0.2-0.3 dB less in this scan. This is partially due to the process of constructing the median profiles: the precipitation was not evenly distributed about the radar at this time, with weaker Z_H (and little if any refreezing signature in Z_{DR}) to the east and southeast of the radar. To alleviate this, profiles were constructed from only the sector in which the refreezing signature appeared; Z_H and Z_{DR} are increased in this case (by about 2 dBZ and 0.2 dB, not shown), but are still lower than in the other three scans. Therefore, there is some indication that larger Z_H values in the cold air beneath the melting layer can lead to a stronger refreezing signature. profiles of ρ_{hv} have a well-pronounced minimum in the melting layer, as

expected. Beneath the melting layer, values sharply increase back to > 0.99, indicating pure raindrops. The values decrease very slightly between about 1000 m AGL and 500 m AGL, coincident with slight increases in Z_{DR} and Z_H. Starting just above 500 m AGL, the ρ_{hv} profiles decrease rapidly in the zone of refreezing and ice generation. Beneath about 300 m AGL, the data are likely contaminated by ground clutter targets (i.e., these "heights" correspond to ranges very close to the radar). The decrease of ρ_{hv} in the refreezing zone can be explained by considering (i) there is a mixture of hydrometeor species, including ice pellets and needles, and (ii) random orientation of needles in the horizontal plane can lead to reduced ρ_{hv}.

The slight increase in Z_H, Z_{DR} and decrease in ρ_{hv} just above the refreezing zone may be due to collision/coalescence processes and/or accretion of supercooled cloud water droplets, leading to larger raindrops. Z_H and Z_{DR} increase owing to larger sizes and oblateness, respectively, and ρ_{hv} decreases very slightly owing to the broadening of the drop size distribution (and an increase in diversity of drop shapes). Collisions and coalescence become more important for larger Z_H; interestingly, the increase in Z_{DR} in this "pure rain" layer is larger for the scans with larger Z_H, consistent with the notion of more efficient collisional processes. Note that larger raindrops nucleate at warmer temperatures than smaller drops, though they generally take longer to freeze (e.g., Pruppacher and Klett 1997; Kumjian et al. 2010). However, with the relatively small Z_H and Z_{DR} values throughout the layer, it is unlikely that a significant increase in raindrop size occurs, and so the increase in nucleation temperature is probably of little effect. Evaporation can be ruled out because (i) soundings indicate saturated conditions, and (ii) Z_H should decrease if evaporation were ongoing, not increase.

Figure 10 presents a genuine RHI scan through the winter storm, taken at 2317 UTC. Note that this corresponds to the time of the 0000 UTC Norman rawinsonde launch, so the temperature and dewpoint profiles in Figure 9 are more representative and should facilitate comparisons with the polarimetric data. Annotated in Fig. 10 are the areas of interest also shown in Fig. 8: the patches of high Z_{DR} aloft (see Andrić et al. 2010 for a discussion of this signature) associated with dendrites, the melting layer bright band, and the refreezing signature of ice generation beneath the melting layer. The refreezing signature in Figure 10, observed as a local maximum in Z_{DR} and minimum in ρ_{hv}, is centered at an altitude of approximately 700 m AGL. This height level is in close agreement to the observed "warming" perturbation in the 0000 UTC sounding temperature profile. Again, it is awaits future calculations to determine the degree to which freezing and/or depositional growth of ice crystals contribute to this warming.

2.3. Refreezing signature. 1 February 2011 case.

The KOUN WSR-88D radar was not properly functioning during this day and we resort to the data collected by the C-band OU-PRIME polarimetric radar belonging to the University of Oklahoma. Very similar refreezing signature is observed at C band for the storm on 1 February 2011. Fig. 11 illustrates reconstructed RHI trough the storm at 0406 UTC along the azimuth 240°. The melting layer bright band is clearly seen at an elevation of about 1.4 km AGL. At a

height of about 500 - 600 m AGL, in the range 0 – 20 km, a secondary maximum in Z_{DR} is evident which is the signature associated with refreezing of supercooled raindrops.

The signature is clearly seen in the vertical profiles of radar variables reconstructed from the slant range dependencies (Fig. 12). Thermodynamic profiles from the 1 February 2011 observed 00z (black) and 12z (gray) Norman soundings are shown in the top left panel in Fig. 12. The refreezing signature is collocated with a sharp decrease in Z_H of about 7-8 dB, and a slight decrease in ρ_{hv}. A possible temperature perturbation is evident in the 12z sounding, with a nearly isothermal layer centered just above the 0406 UTC refreezing zone.

2.4. Refreezing signature. 24 December 2009 case

A similar signature, although less pronounced, was observed during the "Christmas Blizzard" storm on 12/24/2010 (Fig. 13). The C-band OU-PRIME radar data with high resolution were collected during the event.

2.5. Refreezing signature. Discussion.

The refreezing signatures observed in all four storms examined exhibit remarkable similarities listed below.

(1) They occur at the height where air temperature drops below -8°C and where the air becomes subsaturated with respect to water but remains supersaturated with respect to ice.
(2) The onset of Z_{DR} enhancement corresponds to the radar reflectivity factor of about 32 dBZ which decreases by 5 – 7 dB down to the surface.
(3) Typical maximal value of Z_{DR} associated with the signature is between 1 and 1.5 dB.
(4) The Z_{DR} enhancement is accompanied by tangible decrease of the cross-correlation coefficient ρ_{hv}.
(5) In all three storms, ice pellets have been observed on the ground at the time when the refreezing signature was detected.

There is little doubt that the Z_{DR} enhancement is related to vigorous production of anisotropic (most likely columnar) crystals. It is also likely that the signature is associated with massive refreezing of supercooled raindrops because pure freezing rain would never produce such a high Z_{DR} for such a low Z and such a rapid decrease of Z towards the surface. Indeed, typical value of Z_{DR} for Z = 32 dBZ is about 0.5 dB in pure stratiform rain.

The origin of crystal generation remains unknown. One possibility is a very intense Wegener – Bergeron - Findeisen process of ice depositional growth at the expense of water drops in the air which is subsaturated with respect to water and supersaturated with respect to ice. Crystal embryos may include ice nuclei which become active at temperatures below -5°C or small frozen raindrops. More esoteric explanation suggests production of numerous splinters via the Hallett –

Mossop process which is usually active within the temperature range between -8 and -3°C. Possible clumping of frozen droplets may create "dumbbell shape" graupel which is also characterized by enhanced Z_{DR}.

Whatever is the microphysical reason for ice production, practical implications of the observed phenomenon are promising because the signature can be utilized for detection of freezing rain and its transition to ice pellets / sleet.

III. Z_{DR} plums and depolarization streaks.

One of the interesting features we see in the dual polarized observations of winter storms are small regions of high Z_{DR} embedded in the crystal or aggregate layer. These are Z_{DR} "plums" or "blobs" first discussed by Hogan et al. (2002) and Field et al. (2004). These plums usually have lower reflectivity than surrounding areas of lower Z_{DR}. It is believed that they are located in the close proximity of convective updrafts containing graupel and supercooled water. Several examples of from the measurements made by OU-PRIME are illustrated in Figs. 14 – 16. In each example, Z_{DR} in excess of 2 dB is accompanied by reduced Z and ρ_{hv}. These signatures are persistent in time and space as Fig. 15 shows. They also exhibit vertical continuity as can be seen from the series of PPI at different elevations (Fig. 16).

There is growing experimental evidence that weak convective updrafts in winter clouds are capable of generating sufficient electric charge separation to produce tangible electric fields which may orient low-inertia crystals near the tops of such updrafts. Such oriented crystals usually cause well-pronounced effects of depolarization on the propagating radar wave, which manifest themselves as radial streaks of positive and negative Z_{DR} if the radar transmits and receives horizontally (H) and vertically (V) polarized waves simultaneously (Fig. 17). As Ryzhkov and Zrnić (2007) and Hubbert et al. (2010) showed, such radial streaks of Z_{DR} cannot be observed with radars operating with alternate transmission of H and V waves. This explains why Hogan et al. (2002) and Field et al. (2004) did not report such remarkable polarimetric attributes of convective updrafts in their studies performed with the Chilbolton S-band radar operating in the alternate transmission / reception mode.

The episodes of electrification last for several volume scans. An example of such temporal continuity is shown in Fig. 18 for the case of 12/24/2009 blizzard. Depolarization streaks persist for about 3 hours for this case. During the February 1, 2011 event, the streaks were evident in the data for 4.5 hours. It looks like the combination of convective updrafts containing graupel and supercooled water and pristine crystals in the proximity of such updrafts is a necessary attribute of the depolarization signature. It is not observed at lower levels where aggregates usually overwhelms crystals and at very high levels where updrafts are either weak or nonexistent and graupel is not generated. The depolarization signatures were not detected at elevations below 2.4° and above 9.9° as Fig. 19 shows.

IV. Sudden change of precipitation at the surface. "Wandering" bright band. Demise of the melting layer.

Intensive melting and refreezing of hydrometeors can cause significant change in the temperature of environment due to release or absorption of latent heat. This in its turn may lead to rapid local change of precipitation type near the surface. For example, local warming by refreezing of hydrometeors or conduction of enthalpy from relatively "warm" melting particles (which are near 0 ºC) to the subfreezing air may produce local isothermal layers that allow melting particles to survive to the surface. Such diabatic warming in the absence of a warm front is similar in nature to diabatic cooling caused by snow melting, which can lead to rain at the surface with warm, above-zero temperatures suddenly changing to snow (e.g., Wexler et al. 1954). Such sudden changeovers of precipitation type are extremely difficult to forecast (e.g., Kain et al. 2000; Lackmann et al. 2002) and any radar-observed indications of such events are critical for forecasters.

Rapid changeover of the precipitation type near the surface is illustrated in Fig. 19 where the series of RHIs at fixed azimuth 25° is presented from 0332 UTC till 0604 UTC on February 1, 2011. The melting layer descends to the surface at 0420 UTC at the distances beyond 25 km from OU-PRIME. This means sudden change of surface precipitation from freezing rain to wet snow. Such a change is possible if precipitation is intense enough and lasts for certain period of time in order to significantly warm surrounding air which is confirmed by the local increase in radar echo intensity.

Melting layers or bright bands in stratiform precipitation usually have large horizontal extensions. However, if the pocket of warm air is trapped aloft, then the area of snow melting may appear as an isolated "wandering" bright band clearly seen in the time series of RHIs in Fig. 20. One of the surprising findings in the data for all examined winter storms is rapid disintegration and demise of the melting layer aloft as elevated temperature inversion weakens. As opposed to the case of a frontal boundary, in such situation, the melting layer does not touch the ground and disappears aloft. The time series of PPIs showing the demise of the melting layer in the "Christmas Blizzard" case is presented in Fig. 21.

References

Andrić, J., D.S. Zrnić, J.M. Straka, and V.M. Melnikov, 2010: The enhanced Z_{DR} signature in stratiform clouds above melting layer. *Extended Abstracts*, 13th Conf. on Cloud Physics, Amer. Meteor. Soc., Portland, Oregon, P2.89. [available in the online archive of the AMS].

Cao, Q., G. Zhang, E. Brandes, T. Schuur, A. Ryzhkov, and K. Ikeda, 2008: Analysis of video disdrometer and polarimetric radar data to characterize rain microphysics in Oklahoma. *Journal of Applied Meteorology and Climatology,* **47**, 2238 – 2255.

Field, P.R., R.J. Hogan, P.R.A. Brown, A.J. Illingworth, T.W. Choularton, P.H. Kaye, E. Hirst, and R. Greenaway, 2004: Simultaneous radar and aircraft observations of mixed-phase cloud at the 100 m scale. *Quarterly J. Roy. Meteor. Soc.*, **130**, 1877-1904.

Hogan, R., P. Field, A. Illingworth, R. Cotton, and T. Choularton, 2002: Properties of embedded convection in warm-frontal mixed-phase cloud from aircraft and polarimetric radar. *Quart. J. Roy. Meteorol. Soc.,* **128**, 451 – 476.

Hubbert, J.C., S.M. Ellis, M. Dixon, and G. Meymaris, 2010: Modeling, error analysis, and evaluation of dual-polarization variables obtained from simultaneous horizontal and vertical polarization transmit radar. Part II: Experimental data. *J. Atmos. Oceanic Technol.*, **27**, 1599-1607.

Kain, J.S., S.M. Goss, and M.E. Baldwin, 2000: The melting effect as a factor in precipitation-type forecasting. *Wea. Forecasting*, **15**, 700-714.

Kumjian, M.R., S.M. Ganson, and A.V. Ryzhkov, 2010a: Polarimetric characteristics of freezing drops: Theoretical model and observations. *5th European Conf. on Radar in Meteorology and Hydrology*, Sibiu, Romania.

Lackmann, G.M., K. Keeter, L.G. Lee, and M.B. Ek, 2002: Model representation of freezing and melting precipitation: Implcations for winter weather forecasting. *Wea. And Forecasting*, **17**, 1016-1033.

Pruppacher, H., and J. Klett, 1997: *Microphysics of Clouds and Precipitation*. Kluwer Academic

Ryzhkov, A.V., D.S. Zrnić, 2007: Depolarization in ice crystals and its effect on radar polarimetric measurements. *J. Atmos. Oceanic Technol.*, **24**, 1256-1267.

Wexler, R., R.J. Reed, and J. Honig, 1954: Atmospheric cooling by melting snow. *Bull. Amer. Meteor. Soc.*, **35**, 48-51.

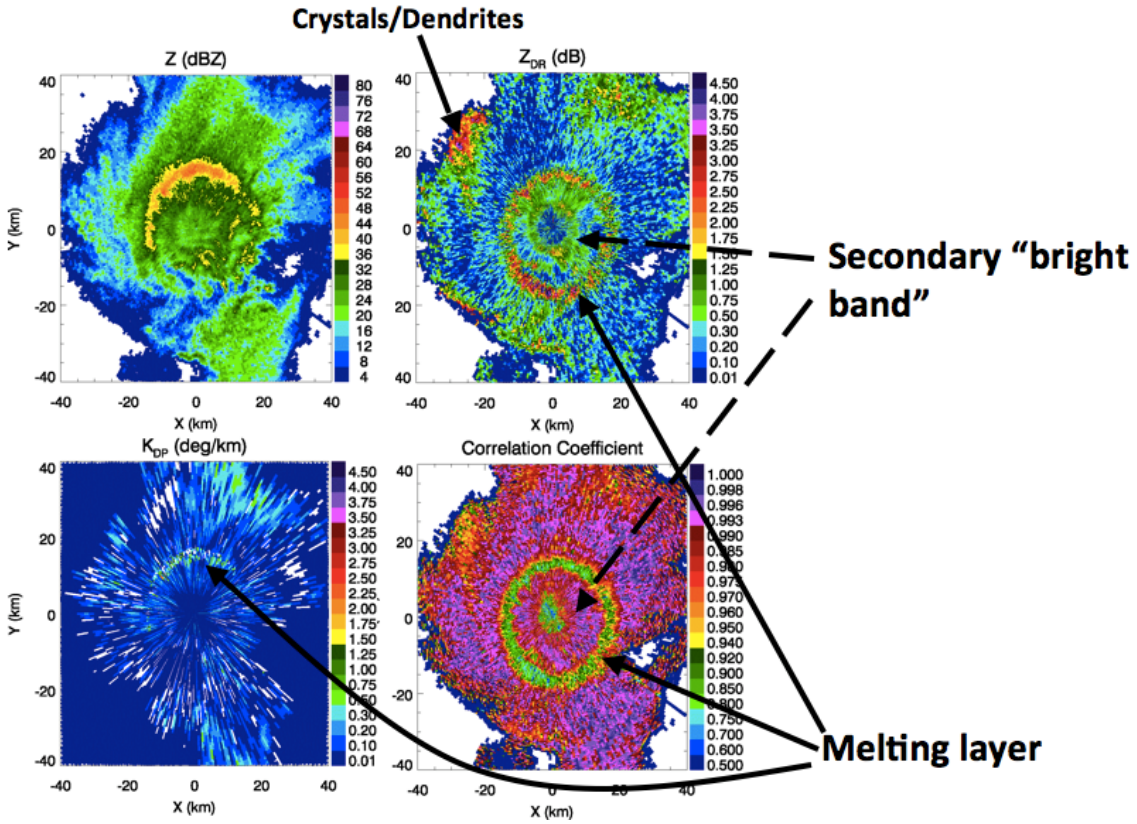

*Fig. 1: KOUN observations from 30 November 2006 at 14** UTC, showing (clockwise from top left panel) Z_H, Z_{DR}, ρ_{hv}, and K_{DP}. Features of interest are annotated: the melting layer bright band signature, a secondary bright band closer to the radar, and dendritic growth of snow crystals at the periphery of the cloud (in Z_{DR}). See text for details.*

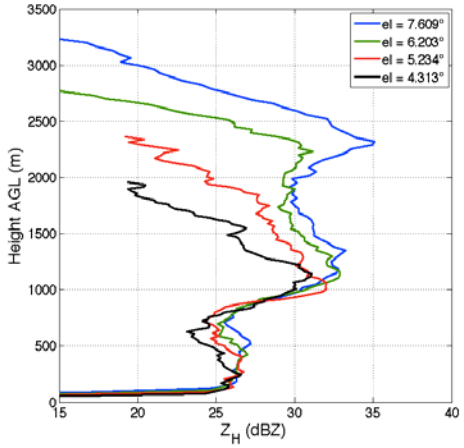

Fig. 2: Median profiles of Z_H from four elevation angles (4.313° in black, 5.234° in red, 6.203° in green, and 7.609° in blue), constructed from the 180° azimuthal sector to the east of KOUN from the volume scan starting at 1358 UTC.

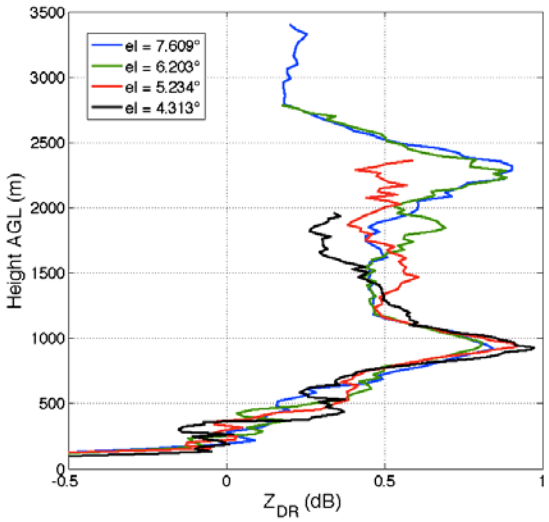

Fig. 3: Same as Fig. 2, but for Z_{DR}.

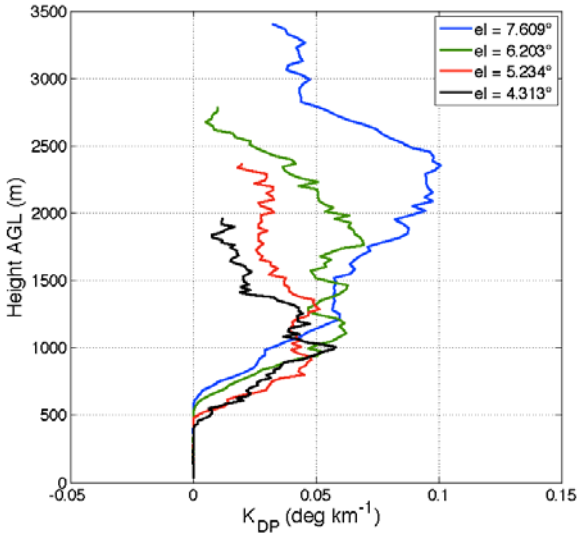

Fig. 4: As in Figs. 2-3, but K_{DP} is shown.

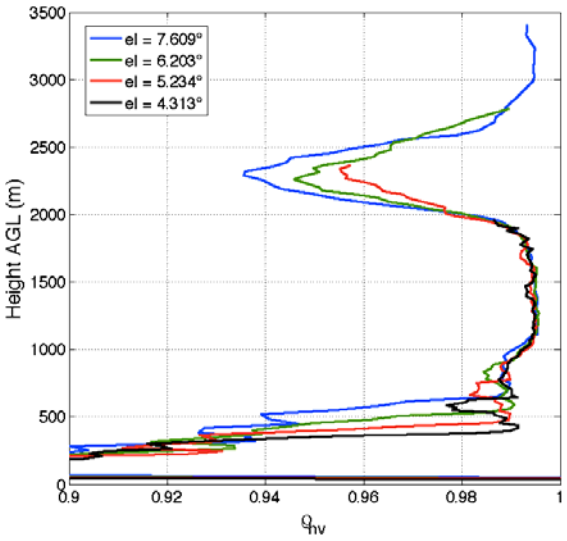

Fig. 5: As in Figs. 2-4, but ρ_{hv} is shown.

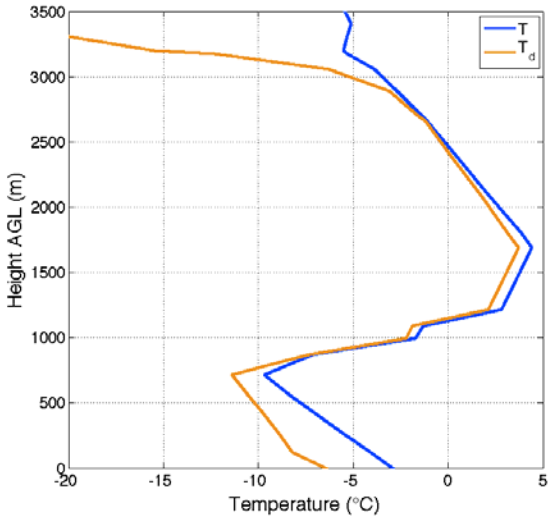

Fig. 6: Observed temperature (blue) and dewpoint temperature (orange) profiles from the 12 UTC Norman sounding on 30 November 2006.

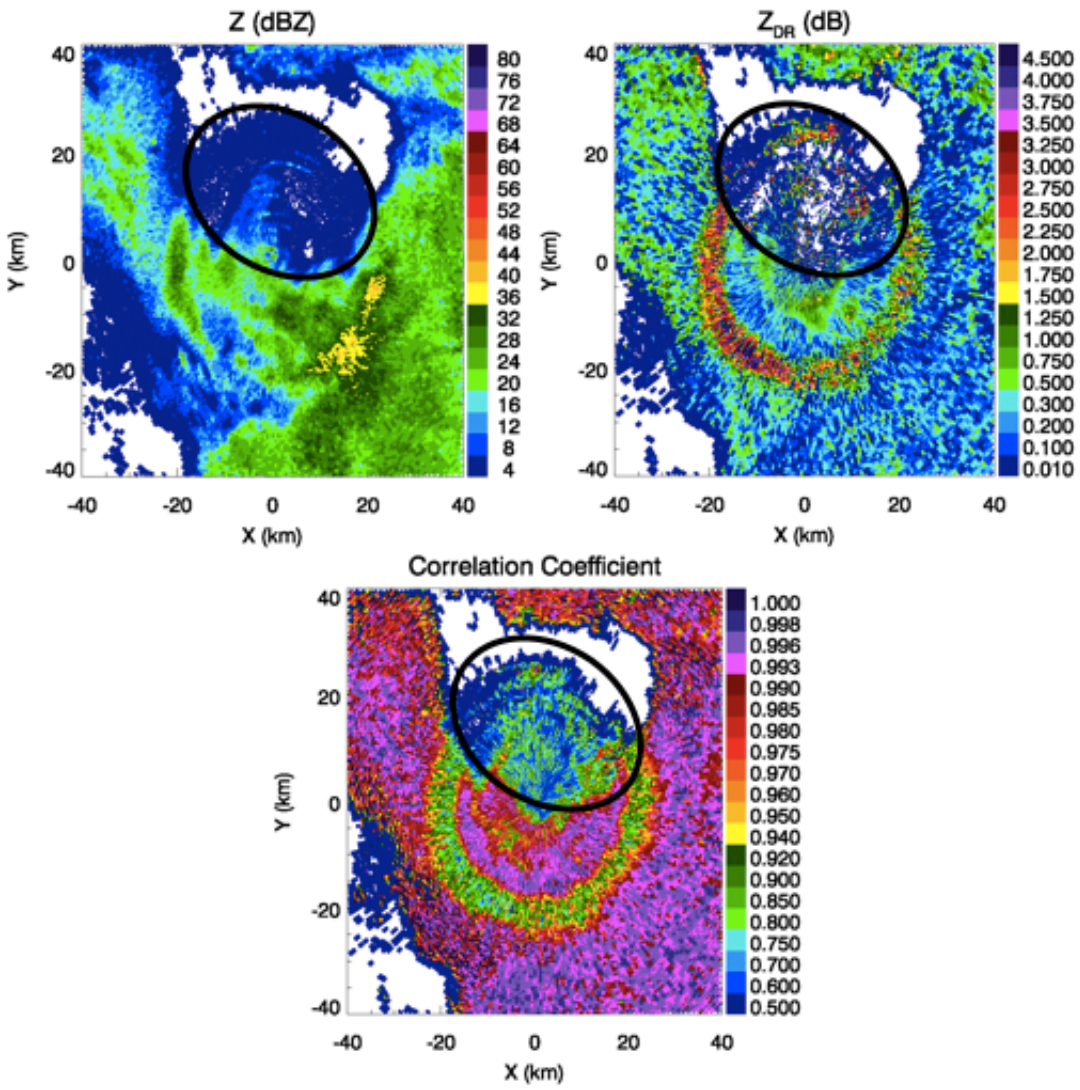

*Fig. 7: Observations of Z_H, Z_{DR}, and ρ_{hv} from 14** UTC on 30 November 2006, with an oval encircling the region lacking a refreezing (or melting layer) signature.*

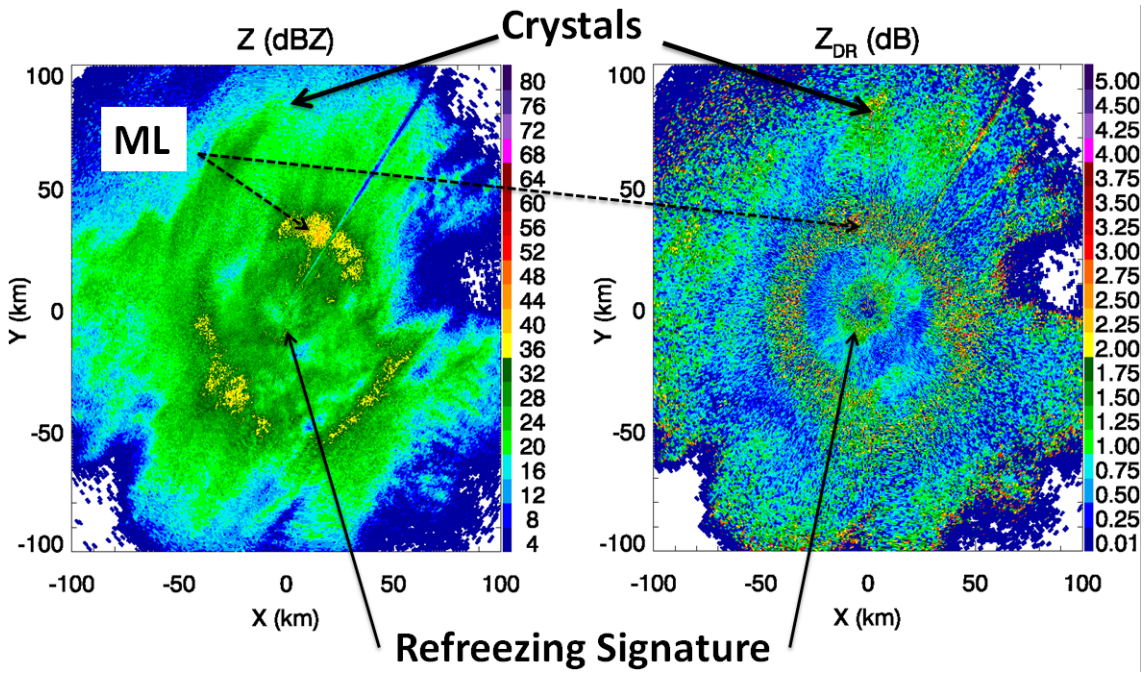

Fig. 8: Z_H and Z_{DR} PPIs from 27 January 2009 at approximately 2005 UTC, taken at 2.4° elevation. Areas of interest are annotated, including anisotropic crystals at the periphery of the storm, the classic melting layer (ML) bright band signature centered at a range of about 45 km from the radar, and a secondary "bright band" signature associated with refreezing centered at about 10 km from the radar. KOUN is located at the center of the image, and all distances are relative to KOUN.

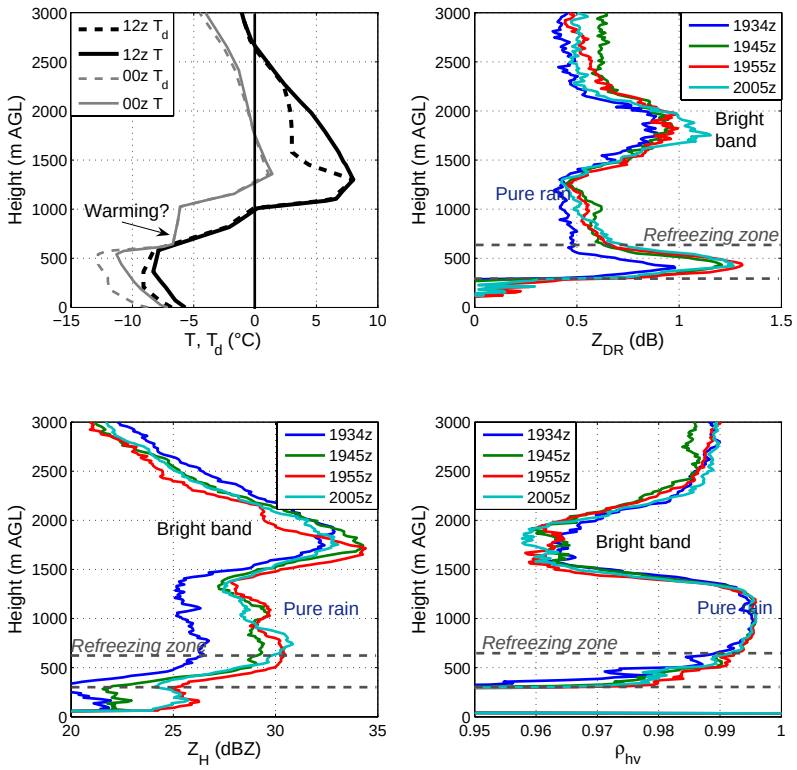

Fig. 9: Quasi-vertical profiles of temperature and dewpoint temperature (top left panel; solid and dashed lines, respectively) observed from the 1200 UTC (black lines) and 0000 UTC (gray lines) soundings on 27-28 January 2009. The remaining three panels show median quasi-vertical profiles of the radar variables (over all 720 azimuths) reconstructed from the 3.3°-elevation scans at 1934 UTC (blue), 1945 UTC (green), 1955 UTC (red), and 2005 UTC (cyan). The radar variables shown are Z_{DR} (top right), Z_H (bottom left), and ρ_{hv} (bottom right).

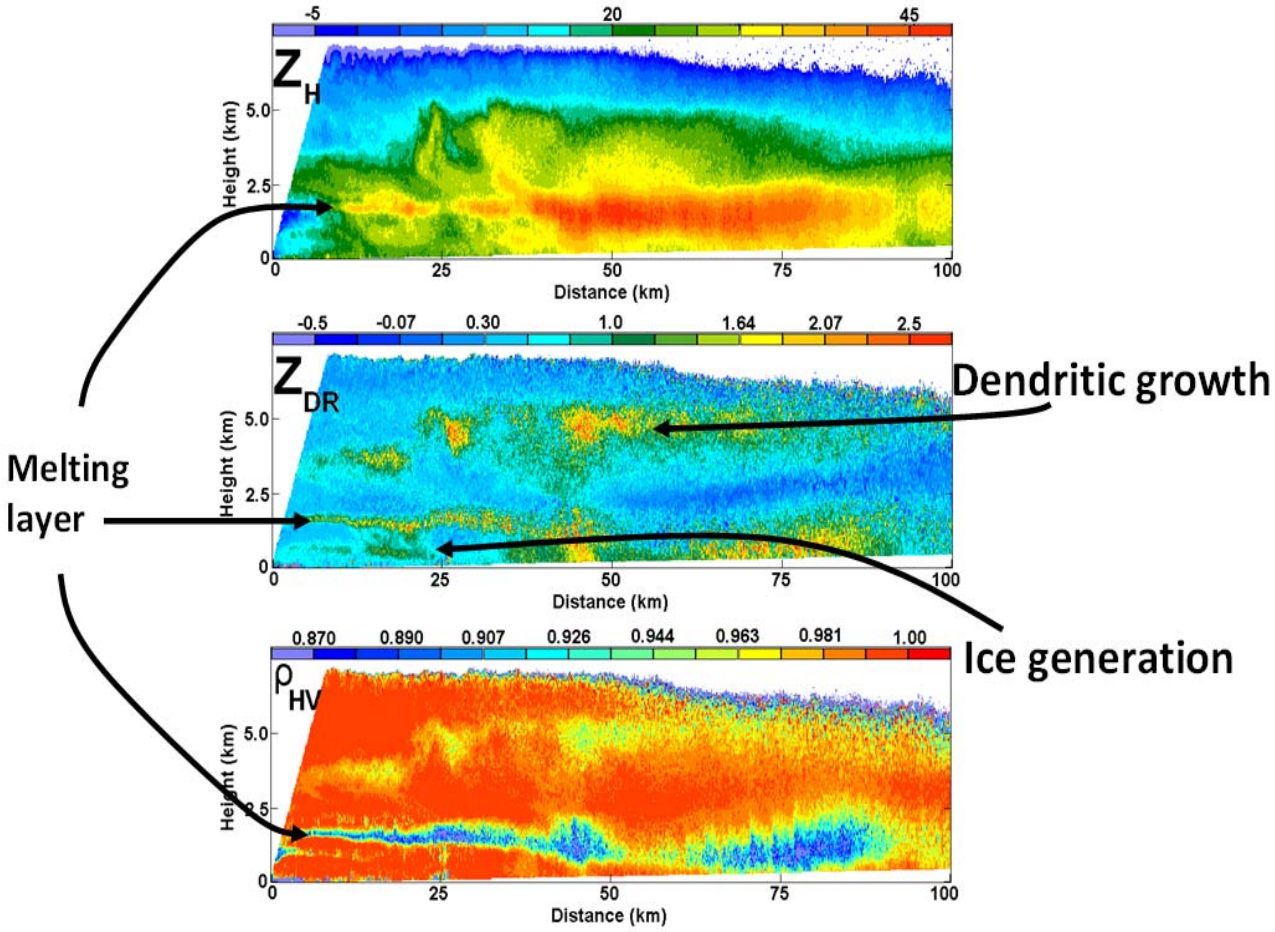

Fig. 10: Three panels showing a genuine RHI scan on 27 January 2009, taken at about 2317 UTC, along the azimuth 181.4°. Note that this RHI is taken during the ascent of the 0000 UTC Norman sounding shown in Figure 9.

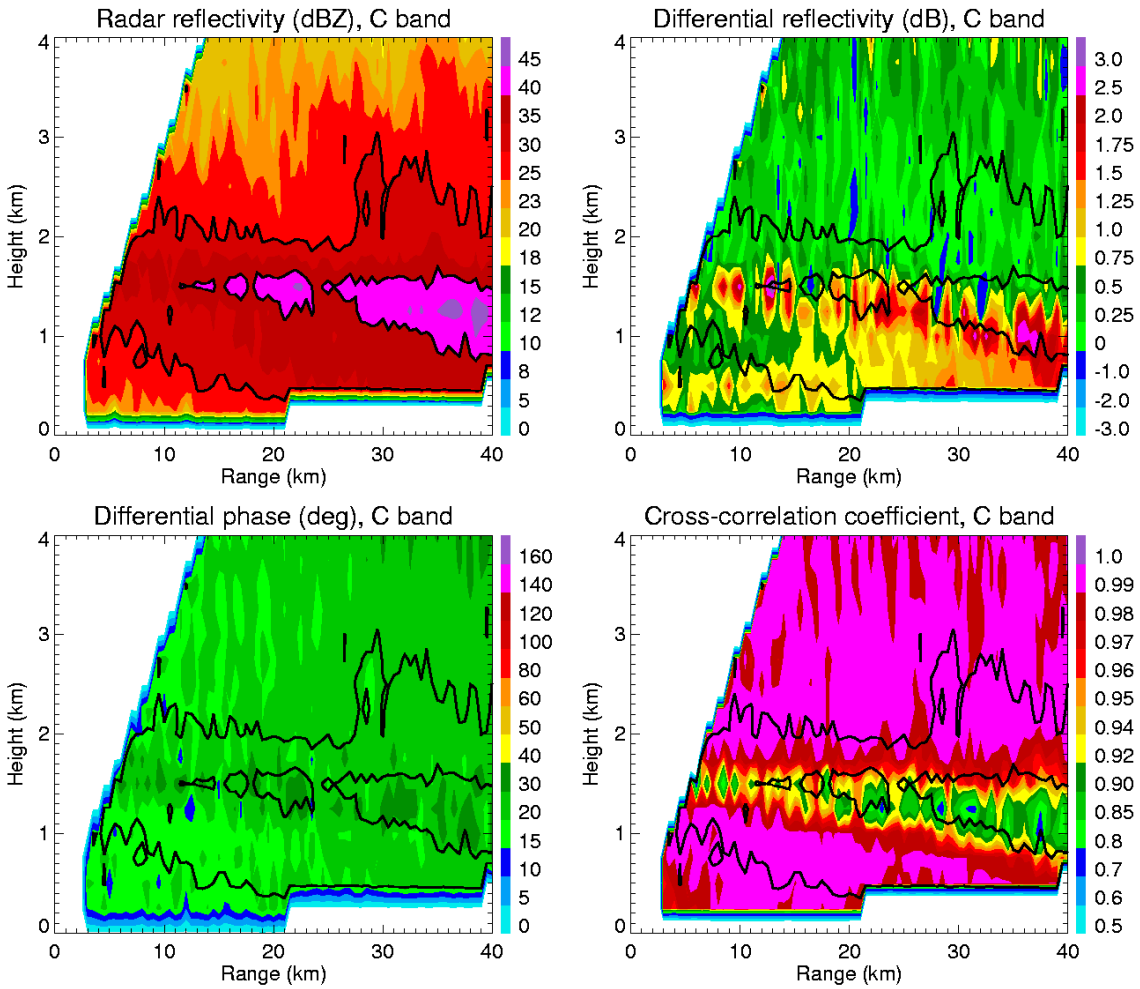

Fig. 11: Reconstructed composite RHI through the winter storm on 1 Feb 2011, at 0406 UTC along the azimuth 240°. Data are collected by C-band OU-PRIME.

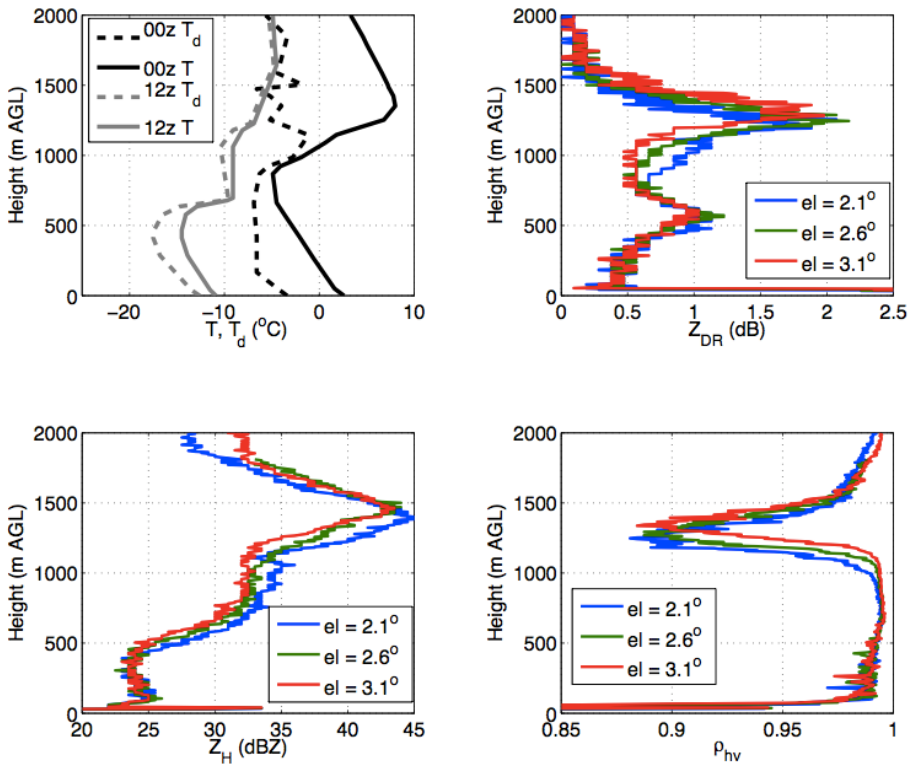

Fig. 12: Quasi-vertical profiles of temperature and dewpoint temperature (top left panel; solid and dashed lines, respectively), Z_{DR} (top right), Z_H (bottom left), and ρ_{hv} (bottom right). Thermodynamic profiles from the 1 February 2011 observed 00z (black) and 12z (gray) Norman soundings. Quasi-vertical profiles of the polarimetric radar variables are constructed from azimuthal medians of constant elevation angle scans (volume scan starting at 0406 UTC; colors indicated in legend) from OU-PRIME.

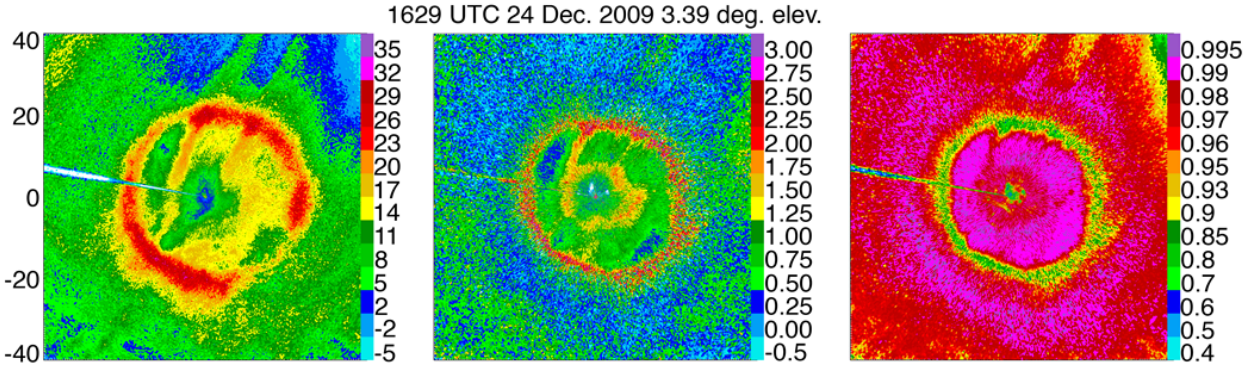

Fig. 13. Evidence of the refreezing signature in the "Christmas Blizzard" storm on 12/24/2009.

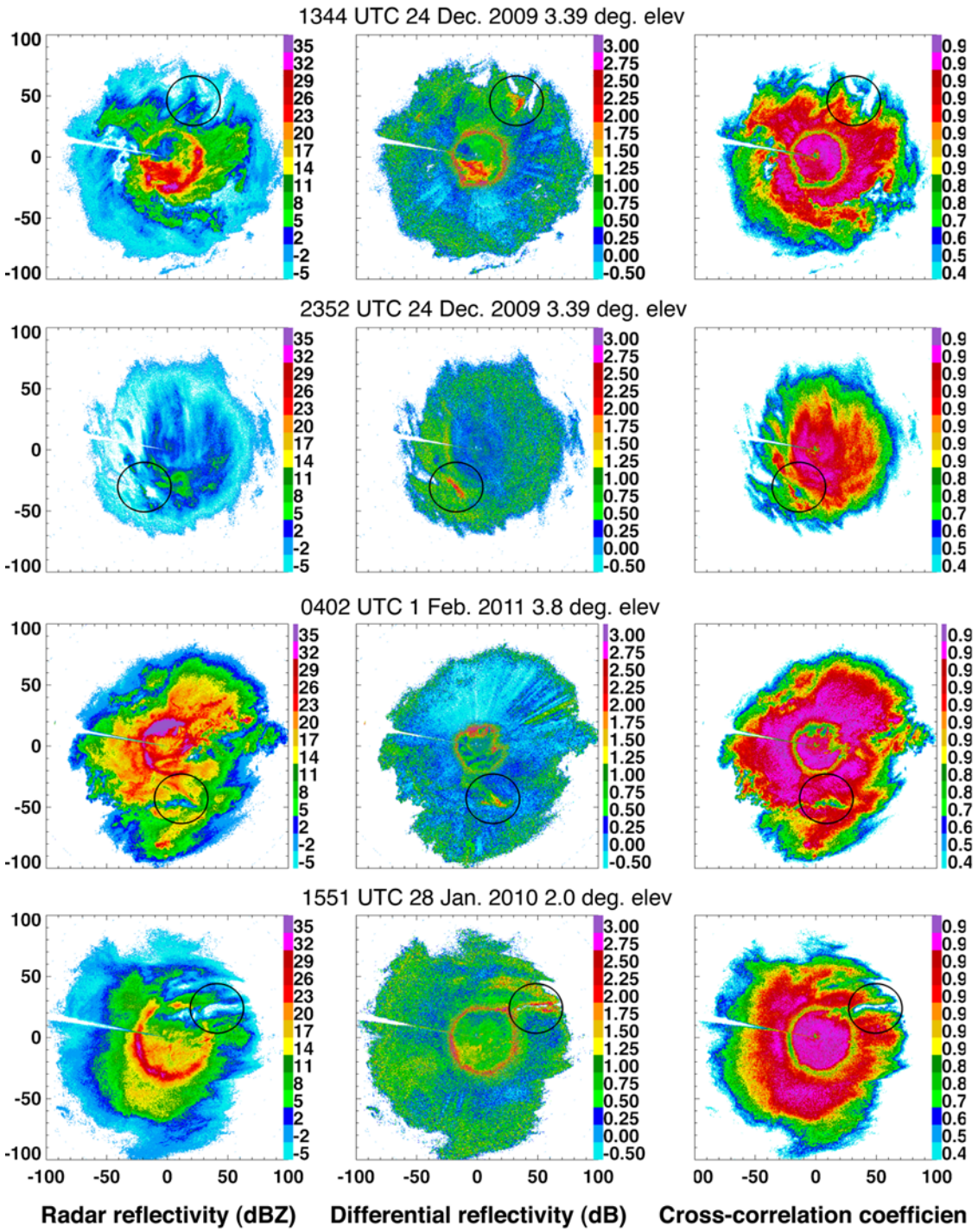

Fig. 14 Examples of Z_{DR} "plums" or "blobs" above the freezing level for three winter storms. The "plums" are enclosed in circles.

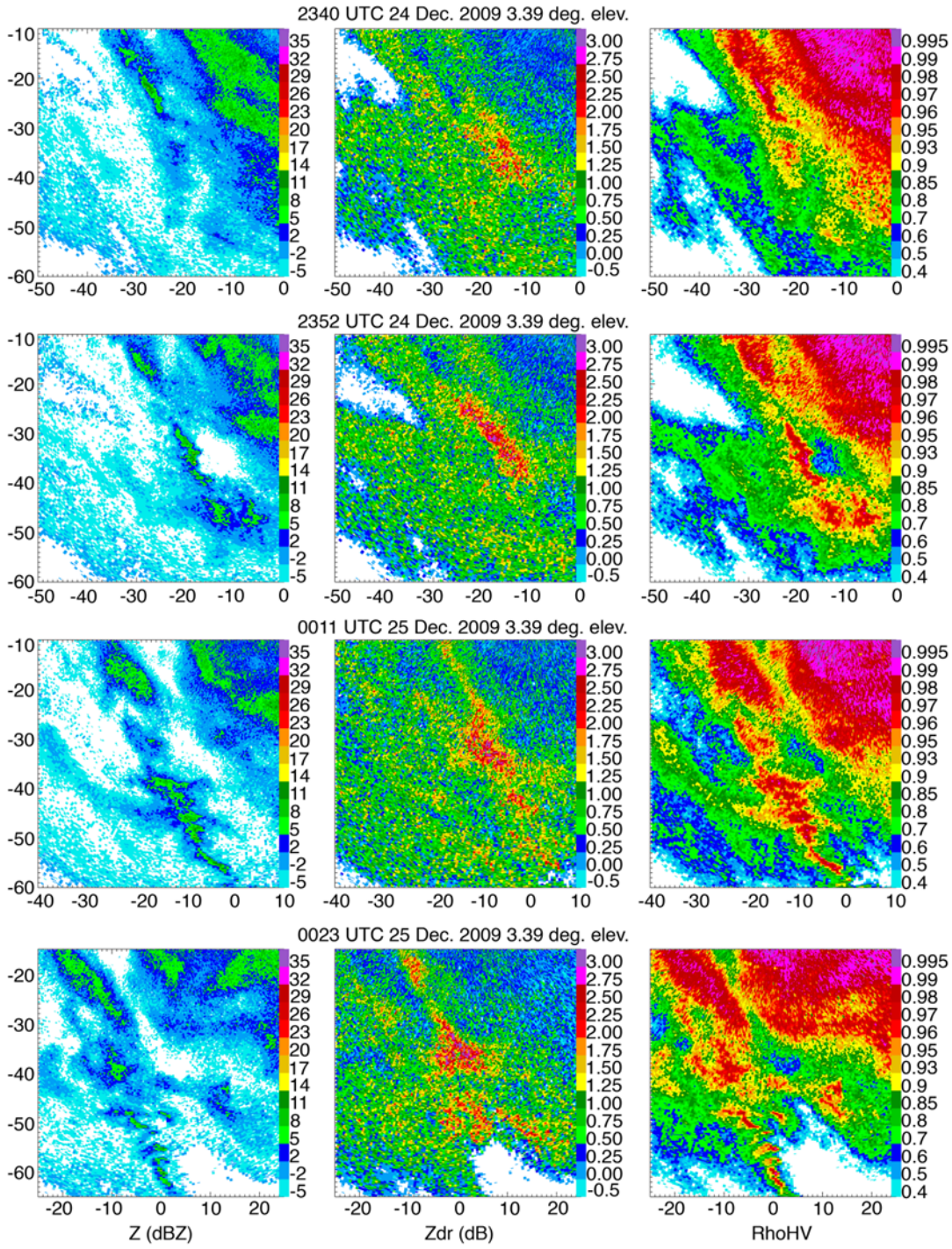

Fig 15. Temporal evolution of a Z_{DR} plum during the "Christmas Blizzard" storm on 12/24/2009. The data are from the C-band OU-PRIME radar.

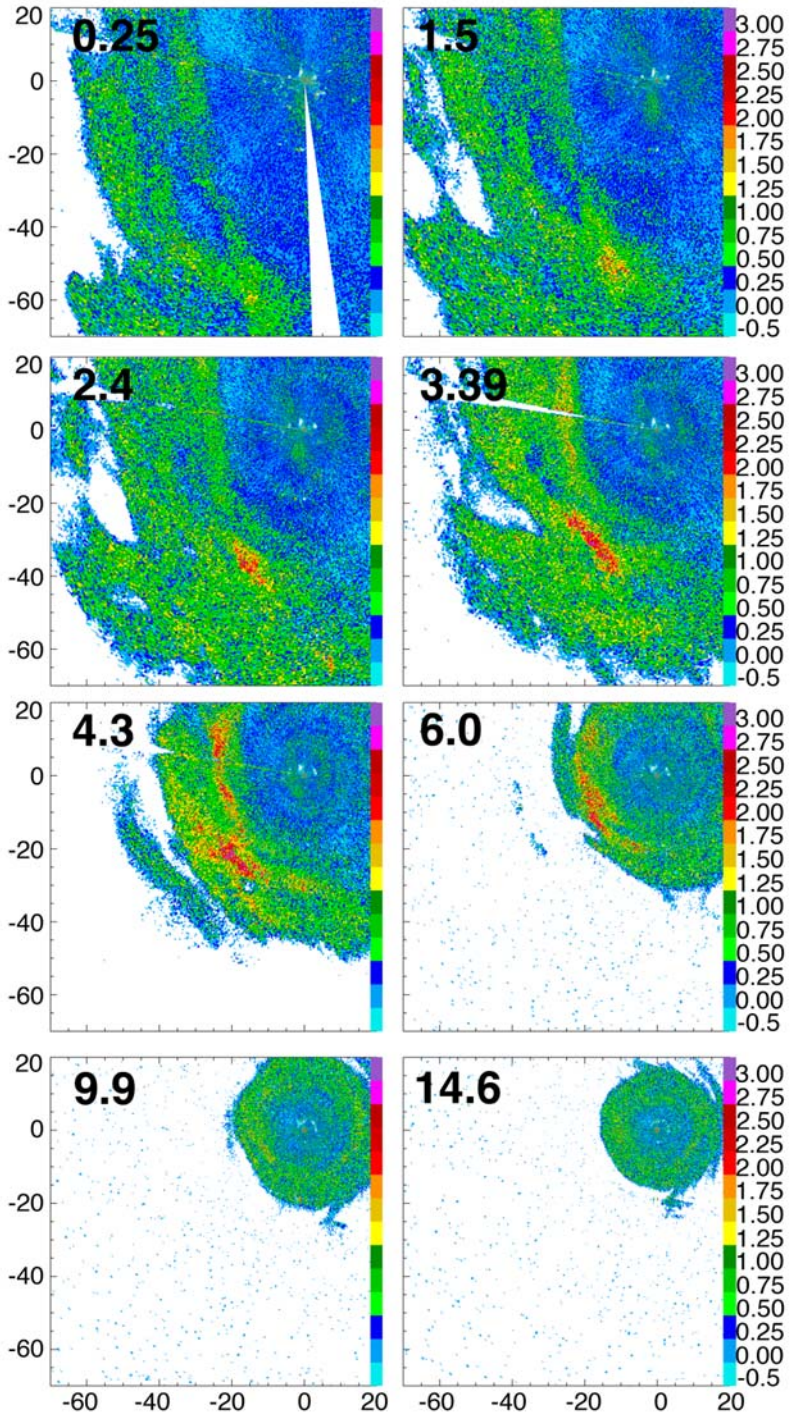

Fig. 16. The Z_{DR} "plums" at different antenna elevations for a single volume scan on 12/24/2009 at 2352 UTC. The data are collected by the OU-PRIME radar.

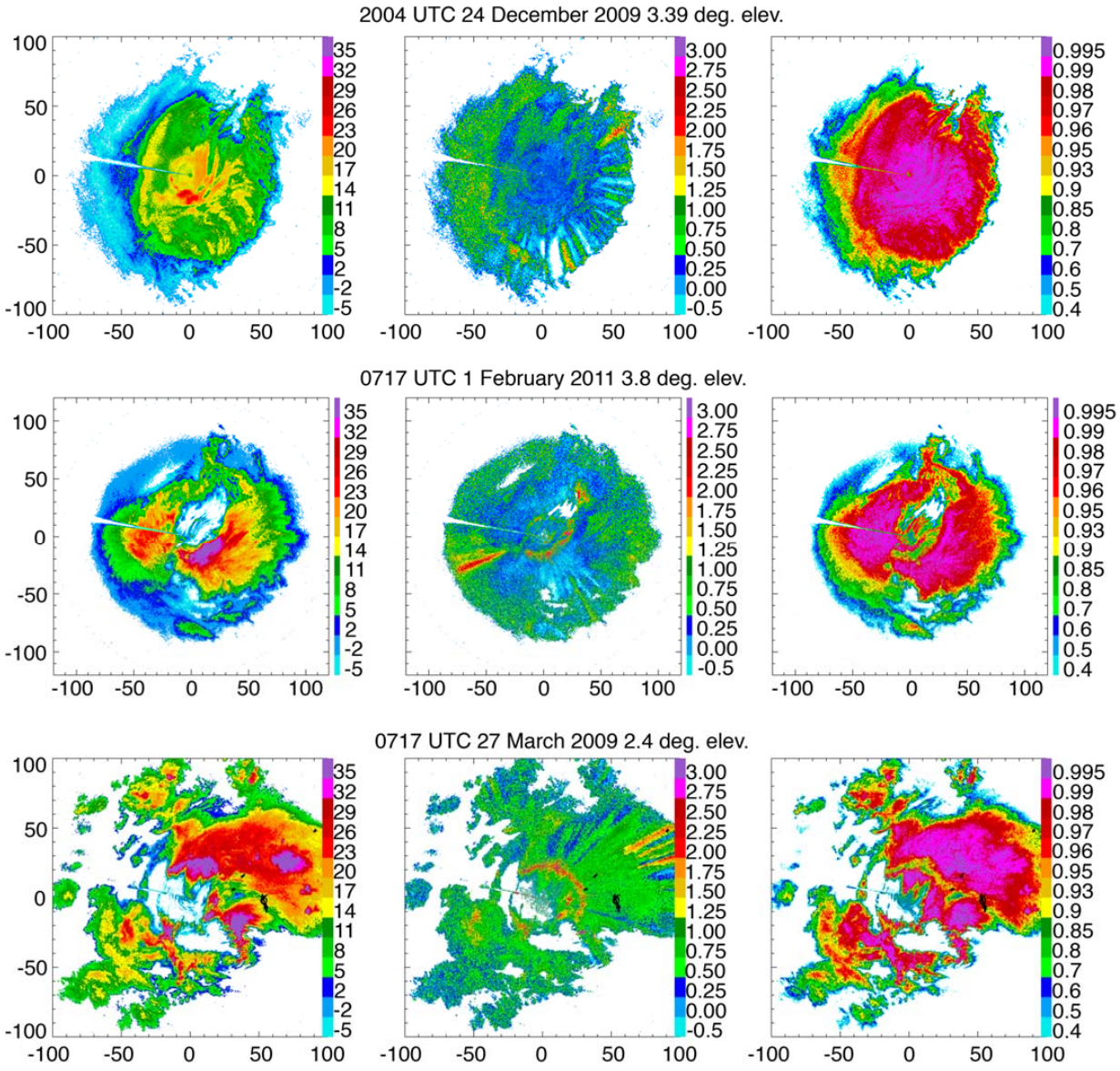

Fig. 17. Examples of Z_{DR} depolarization streaks in three winter storms. The streaks are caused by electrification near the tops of weak convective updrafts.

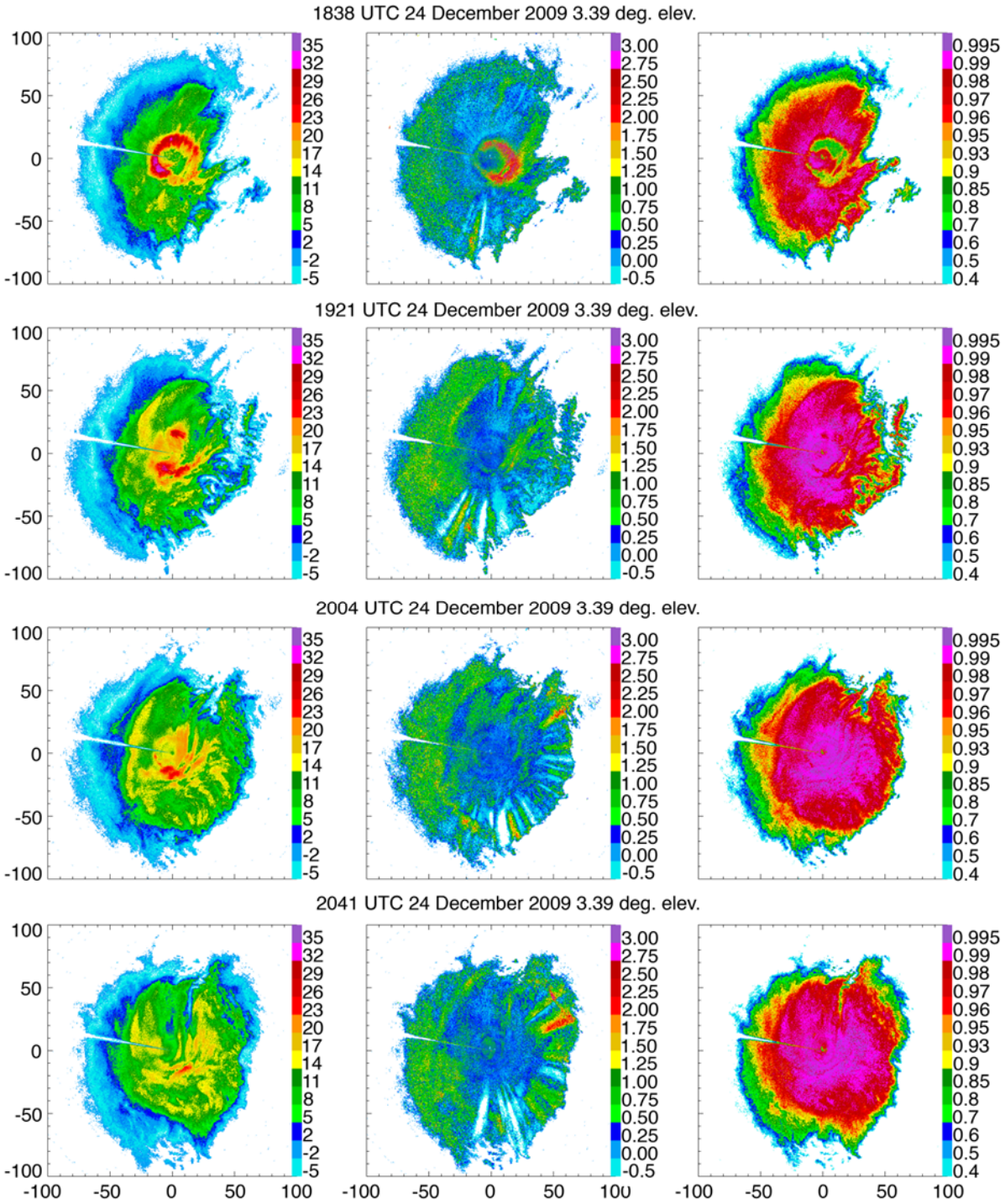

Fig. 18. Temporal evolution of the Z_{DR} depolarization streaks during the "Christmas Blizzard" storm on 12/24/2009.

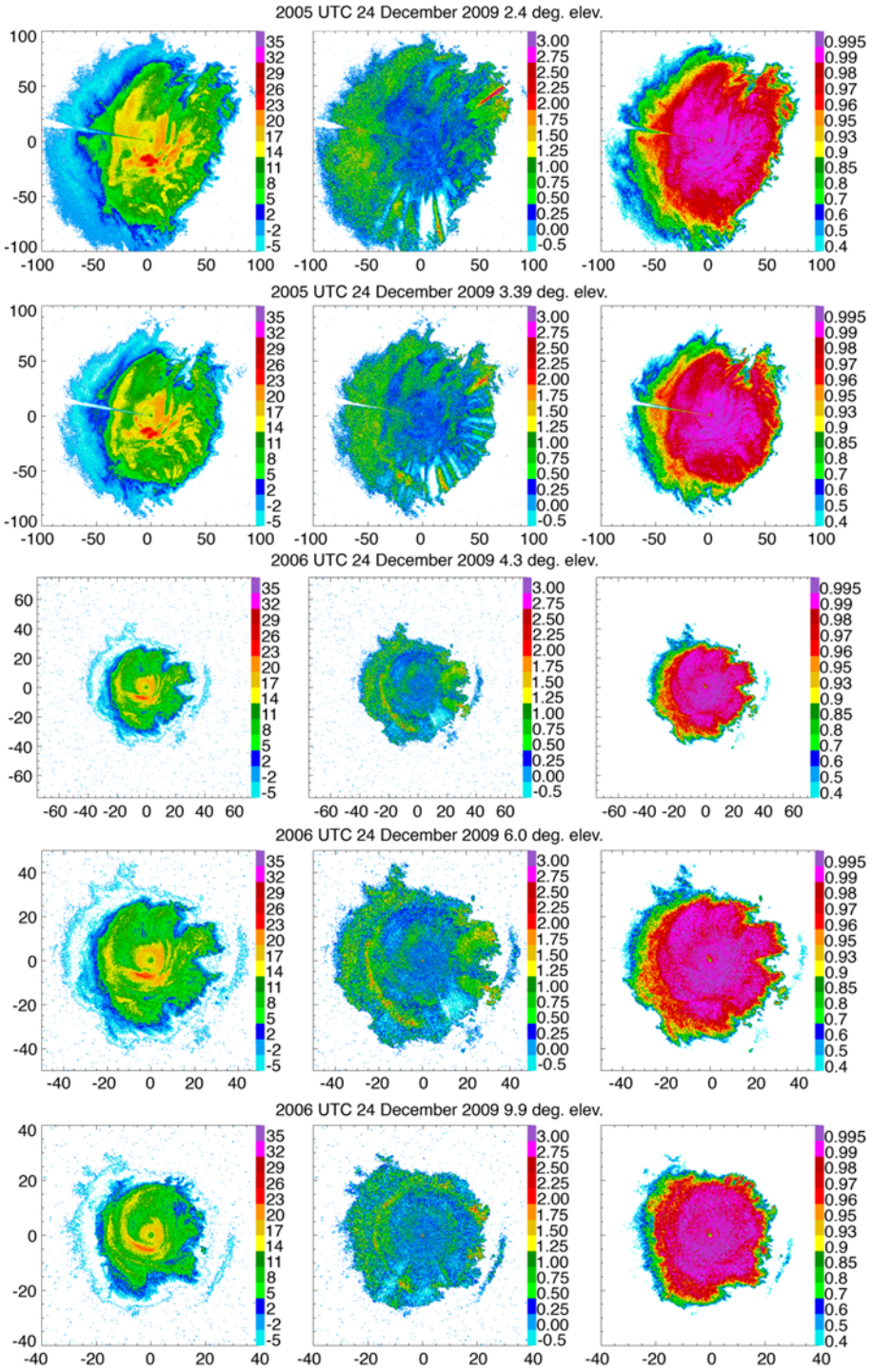

Fig. 18. Depolarization streaks at different elevation angles for a single volume scan during the "Christmas Blizzard" storm on 12/24/2009 at 2004 UTC.

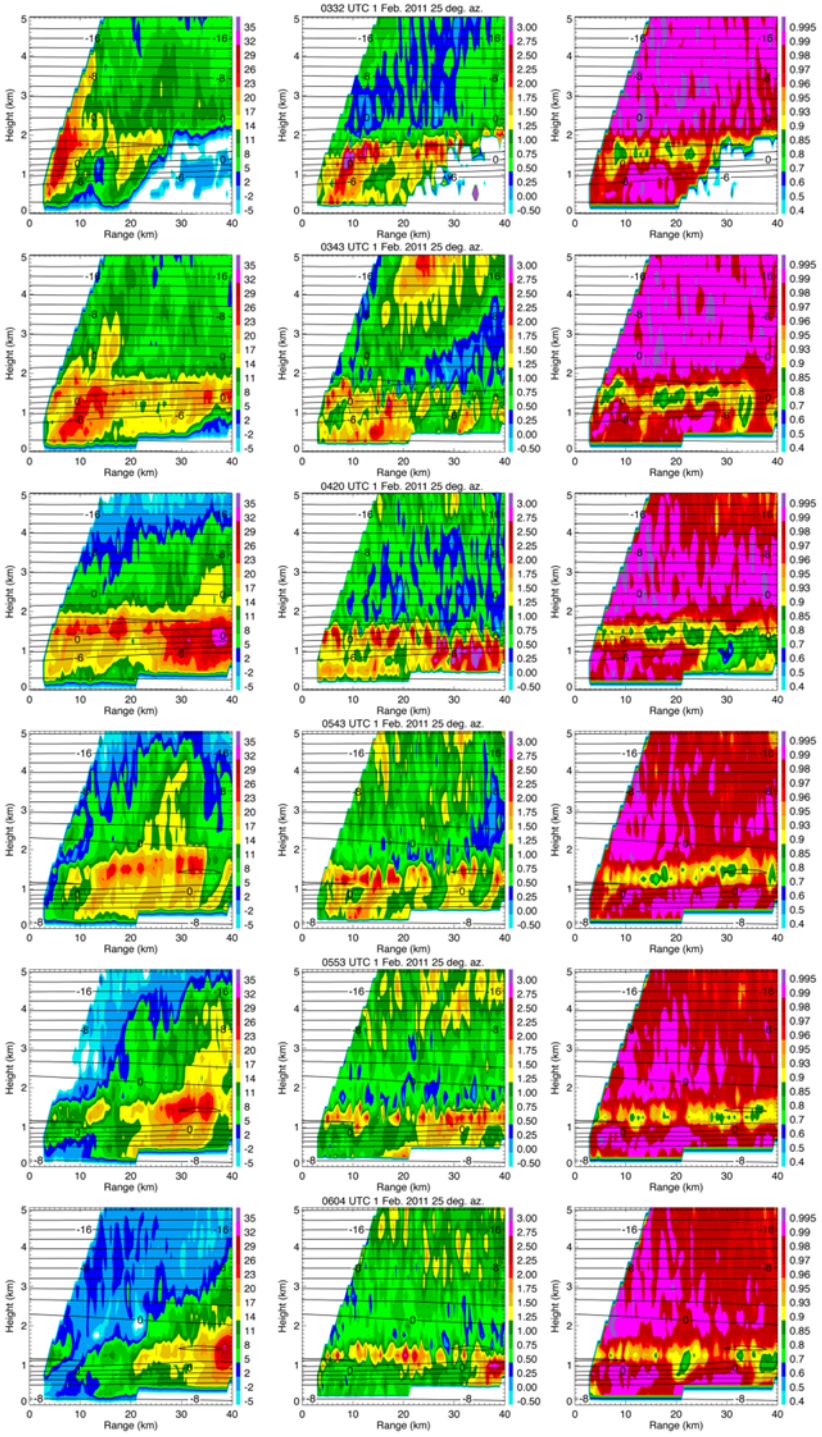

Fig. 19. Illustration of sudden change in precipitation type near the surface for the storm on February 1, 2011. Massive amount of wet snow falls on the ground at 0420 UTC at ranges exceeding 25 km from OU-PRIME.

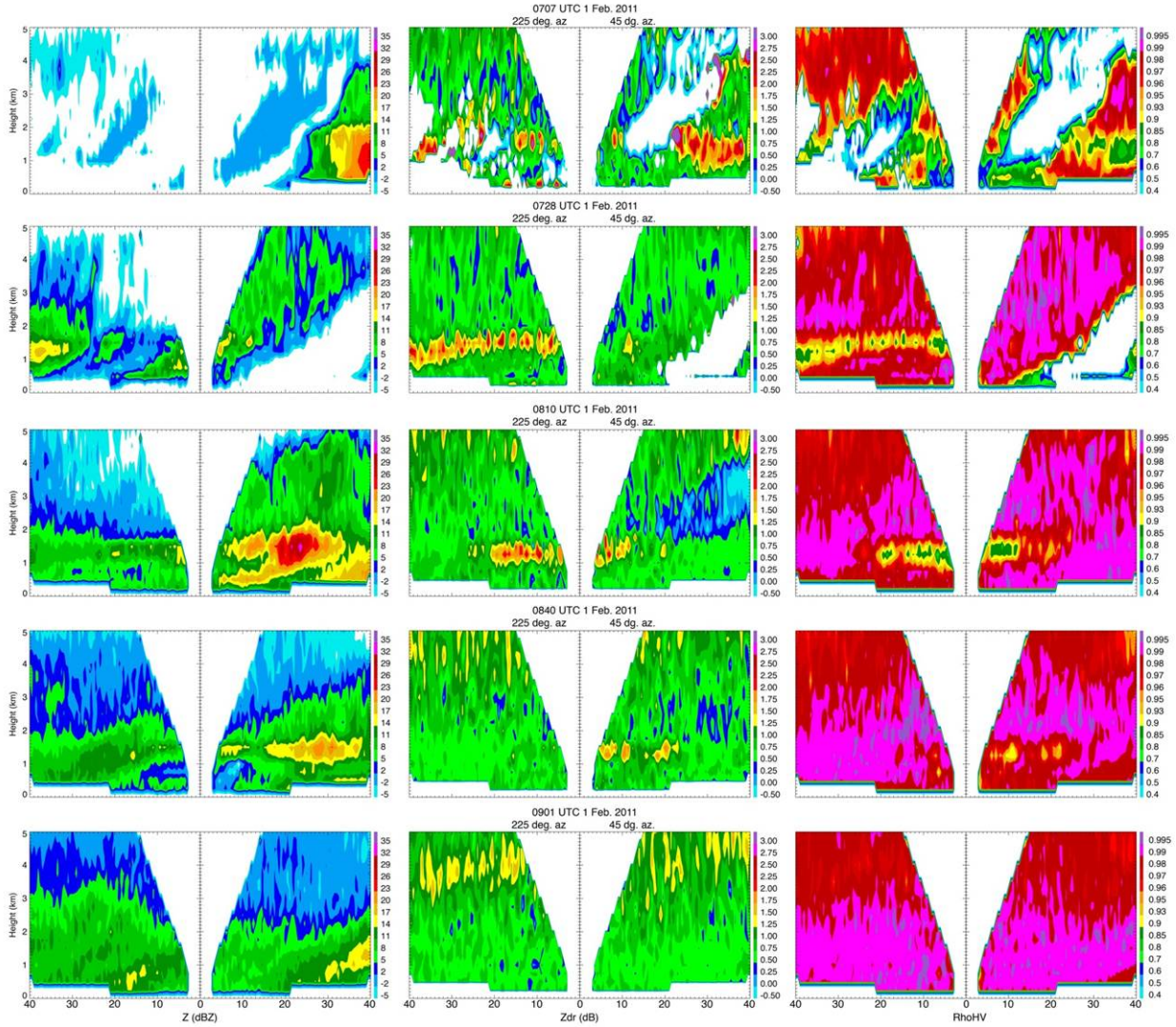

Fig. 20. Illustration of "wandering" and isolated bright band.

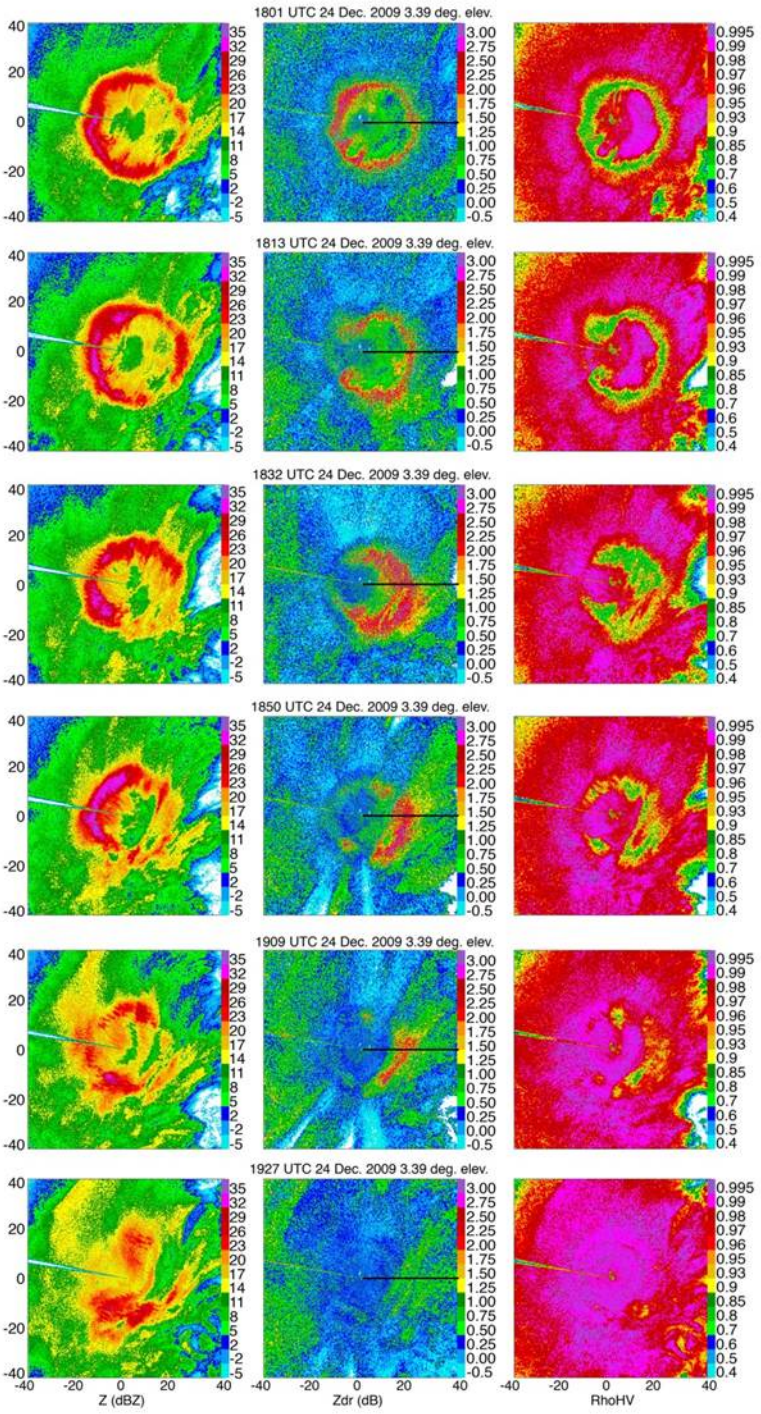

Fig. 21. Temporal evolution of the melting layer signature during the "Christmas Blizzard" storm on 12/24/2009.